Human Cytomegalovirus mir-UL70-3p downregulates the H_2O_2 induced apoptosis in HEK293T cells by targeting the Modulator of Apoptosis-1 (MOAP1)

Abhishek Pandeya
Babasaheb Bhimrao Ambedkar University
Anup Mishra
Babasaheb Bhimrao Ambedkar University
Raj Kumar Khalko
Babasaheb Bhimrao Ambedkar University
Sukhveer Singh
CSIR-Indian Institute of Toxicology Research
Nishant Singh
CSIR-Indian Institute of Toxicology Research
Sanjay Yadav
All India Institute of Medical Sciences Raebareli
Sudipta Saha
Babasaheb Bhimrao Ambedkar University
Sangeeta Saxena
Babasaheb Bhimrao Ambedkar University
Sunil Babu Gosipatala (gsbabu@bbau.ac.in)
Babasaheb Bhimrao Ambedkar University https://orcid.org/0000-0002-5377-817X

Research Article

Keywords: Apoptosis, HCMV, miR-UL70-3p, Modulator of Apoptosis-1

Posted Date: May 17th, 2021

DOI: https://doi.org/10.21203/rs.3.rs-504584/v1

Abstract

Human Cytomegalovirus (HCMV), a prototypic member of the *Beta-herpesvirinae* subfamily, mainly responsible for congenital disabilities in newborns, cause opportunistic infections in immunocompromised individuals. Its seroprevalence varies across the globe ranging from 50–70 percent in developed countries to 90–100 percent in developing countries. Causing latent infections in the immunocompetent host suggests that it employs several strategies to escape the wrath of the host's antiviral mechanisms. Apoptosis is an innate cellular response to viral infection, and downregulation of this mechanism by HCMV is a well-established phenomenon. HCMV utilizes its proteins, RNA and miRNA in regulating this response to establish a productive infection in the host. The role of HCMV miRNAs on cellular apoptosis is very interesting, where some miRNAs downregulate but a few upregulate this process. In the present study, we report the antiapoptotic activity of HCMV miRNA, miR-UL-70-3p, on H_2O_2 induced apoptosis in HEK293T cells. The ectopic expression of this HCMV miRNA in HEK293T cells downregulate the apoptosis, and continuing studies reveal that the proapoptotic gene, Modulator of Apoptosis Protein-1 (MOAP1), is a functional target for this miRNA. We verified the functionality of the binding site predicted in the 3'UTR of MOAP1 in our earlier studies through dual luciferase-based assays using both the wild and mutant 3'UTR's of MOAP1. The MOAP1 protein levels were significantly downregulated by the miR-UL70-3p, suggesting that the MOAP1 mRNA was degraded after binding with the miR-UL70-3p. Further, the extent of MOAP1 mRNA and its protein inhibitions by HCMV miR-UL70-3p and siRNA of MOAP1 were compared and found that the siRNA of MOAP1 inhibits 69.52 percent of mRNA and 35.67 percent of MOAP1 protein; while the miR-UL70-3p inhibits 46.66 percent MOAP1 mRNA and 21.05 percent MOAP1 protein. Though the inhibitory activity of miR-UL70-3p is not equal to the siRNA of MOAP1, but it was significant enough in reversing the H_2O_2 induced apoptosis in HEK293T cells. These results confirm that hcmv-miR-UL70-3p downregulates H_2O_2 induced apoptosis in HEK293T cells by targeting the 3'UTR of MOAP1 mRNA.

Introduction

Human Cytomegalovirus (HCMV) is a ubiquitous human pathogen belonging to the *Betaherpesvirinae* subfamily, which is able to maintain latent infection that persists throughout the life of the host [1]. It shows subclinical symptoms in an immunocompetent host but causes significant mortality and morbidity in infants and immunocompromised hosts. It is an enveloped DNA virus (≅ 230Kb) encoding more than 170 proteins and numerous long and small non-coding RNAs, making it the largest among the herpesviruses [2–4]. The genome of HCMV is divided into two segments, designated as UL (unique long) and US (unique short), bounded by inverted repeats [5] and contains ~ 150 open reading frames that encode proteins [6]. The gene expressions in this virus occur in temporal order; i.e., the first set of viral gene products are classified as immediate early genes (IE), followed by the expression of early genes (E), and finally, the late gene (L) products. These gene products help the virus in causing latent infections by evading the host effective immune responses. Apoptosis, an innate antiviral immune response, is also inhibited by the viral proteins and miRNAs that helps in establishing and maintaining the latency in the

infected host. HCMV encodes anti-apoptotic proteins through both the US [US4, US28] and UL [UL37, UL38 and UL144] regions of its genome [7, 8]. The antiapoptotic proteins of HCMV, a viral inhibitor of caspase-8- induced apoptosis (vICA/pUL36), and mitochondria localized inhibitor of apoptosis (vMIA/pUL37X1) interferes in the cellular apoptosis by targeting pro-caspase 8 and Bcl2, respectively [9]. Further, a non-coding RNA of HCMV, Beta 2.7, also plays an anti-apoptotic role by interacting with mitochondrial complex I to maintain a high ATP production level preventing the stress-induced re-localisation of retinoid/interferon-induced mortality-19 protein, GRIM-19 [10]. In addition to the proteins/RNA, HCMV also encodes miRNAs, which block/downregulate cellular apoptosis by targeting the proapoptotic genes [11, 12]. As per the latest miRbase, HCMV is reported to encode 26 mature miRNAs expressed during both latent and lytic infections [13–16], known to regulate many cellular pathways, including the immune responses, cytokine production and apoptosis. Once it comes to the regulation of apoptosis by the HCMV miRNAs, it has been observed that some of the miRNAs downregulate the cellular apoptosis, for example, the miRNA's, miR-UL148D [17], miR-UL36-5p [12], whereas hcmv-miR-US22-5p and miR-US-25-15p has been reported to aggravate the apoptosis [18, 19]. miR-US22-5p target autophagy-related 5 (ATG5) and modulate apoptosis [20], miR-US25–1-5p target 5'UTR of BRCC3 (BRCA1/BRCA2-containing complex subunit 3) to modulate apoptosis in oxidised LDL promoted endothelial cells [21], miR-US4-5p target PAK2 (p21-activated kinase 2) to modulate apoptosis, miR-US29-5p another HCMV miRNA that targets ATG5 to regulate apoptosis [19]. Further, by performing *in silico* studies, we predicted the antiapoptotic role of HCMV miR-UL70-3p [22]. In this present study, we demonstrate the antiapoptotic activity of the miRNA in *in vitro s*tudies and proved the modulator of apoptosis 1 (MOAP1) mRNA as a functional target for this miRNA.

Materials And Methods

Cell Lines and Cell culture: HEK293T cell lines were procured from American Type Cell Culture (ATCC, USA) and grown in Dulbecco's Modified Eagle Media (Gibco) supplemented with 10% (v/v) Fetal Bovine Serum (Gibco, Brazil origin) and 1% antibiotic and antimycotic (Gibco). Cells were incubated at 37°C supplemented with 5% CO_2 in a humidified atmosphere and were routinely passaged after confluency reached up to 80%. The cells were routinely tested for mycoplasma infections.

HCMV miRNA mimic, Inhibitors and siRNA: The hcmv-miR-UL70-3p mimic and its inhibitor were procured from Ambion, Life Technologies (Assay ID: MC11312, Cat No: 4464066; MH11312 cat No: 4464084). The sequence of hcmv-miR-UL70-3p: 5´ ggg gau ggg cug gcg cgc gg 3´ . The siRNA of MOAP1 was procured from the Integrated DNA Technologies, Inc., Coralville, IA, USA (cat no: hs.Ri. MOAP1.13.1) and the sequence of siRNA of MOAP1 is 5´ agu aua uag acu guu cua ccu uca ugc 3´.

Transfection and co-transfection: The miR-UL70-3p and its inhibitor were transfected with Dharmafect1 No T-2001-03 (Dharmacon, USA), whereas all the co-transfection experiments were carried out with Lipofectamine 3000 as per the manufacturer's protocol (L3000008- Invitrogen, USA).

Vectors:

The 3' UTR of MOAP1 was cloned in the pEZX-MT06 vector of Genecopoeia, USA, (cat No: HmiT016794-MT06 & Cat No: Cmi000001-MT06), which contains firefly luciferase as the reporter gene (controlled by the SV40 promoter) and Renilla luciferase as the tracking gene (Controlled by the CMV promoter).

4',6-Diamidino-2-phenylindole (DAPI) staining:

Apoptotic cell nuclei were observed by staining with 4',6-diamidino-2-phenylindole (DAPI) (Himedia Cat No: TC 229) under the fluorescent Microscope using the blue filter at emission/ excitation 358nm ⁄ 461nm. (Axiovert A1-Carl Zeiss-Jena- Germany) as per the protocol mentioned in Fig 1.

Image analysis:

The apoptotic cell nuclei and their condensation were analysed through ImageJ ver. 1.53 (National Institute of Health, Bethesda, MD). In brief, a nuclear morphology measurement, 16-bit photomicrographs of DAPI stained nuclei were converted to the 8-bit image before being the auto threshold to a binary photo using the default method “Make Binary” function in ImageJ. Touching cell nuclei were separated by the “watershed” function, and small fragments of nuclei were discarded on the basis of the area by the “analyzing particle” function. The latter function also provided other morphological parameters, including nuclear area, circumference, and form factor. By comparing the total numbers of cell nuclei obtained with watershed, an estimated percentage of apoptotic cells were computed by human intervention as the number of apoptotic cell nuclei (irregular shape and degraded shape)/ the total number of DAPI stained nuclei (with watershed) * 100, which provided the average percentage of apoptotic cells in each and every experimental setup.

Caspase-Glo 3/7 assay: The apoptotic induction and inhibition were assessed via Caspase-Glo 3/7 assay kit from Promega (Madison, WI, USA Cat No: G8090) using the luminometer (GloMax® Navigator System, Promega). Briefly, the cells were seeded in 96 well white plates followed by overnight incubation. The HEK293T cells transfected with 30nM of hcmv-miR-UL70-3p & its inhibitor was treated with 0.4 mM H_2O_2. The culture plate containing the cells were removed from the incubator and equilibrated at room temperature for 30 min. 100µL of Caspase-Glo reagent was added to each well and gently mixed in a plate shaker. The plate was then incubated at room temperature for 2 hrs. Luminescence was read using the Luminometer (GloMax® Navigator System, Promega). Caspase 3 and 7 activity was measured using raw values of luminescence to obtain a relative to control value. The final caspase activity was calculated by averaging three replicates from two independent experiments.

Flow Cytometry:

HEK293T cells were cultured in a 6-well plate followed by transfection, using DharmaFACT1 (Dharmacon), with 30 nM of miR-UL-70-3p and its inhibitor. Apoptosis was induced by treatment with 0.4 mM concentration of H_2O_2 at 24 hrs post-transfection. After 6 hrs of incubation, cells were washed with PBS, pelleted, and then incubated with 5µL of Annexin-V conjugated with Alexa Fluor 488 (Life Technologies Cat No: A13201) along with the 100 µL of Annexin Binding Buffer for 15 min in the dark.

Then, samples were incubated with the 5µL of Propidium Iodide; (Invitrogen; Cat No: P1304MP respectively) in the dark for 10 min. Then samples were analyzed by diluting the cells with 400µL of 1X binding buffer by Flow Cytometry using FACS Canto II and FACSDiva software (Becton Dickinson Biosciences). The data represents the percentage of apoptotic cells in Q2 and Q4 quadrants, in which Q4 shows cell population having Annexin V^+ and PI^- demonstrating early apoptosis, whereas Q2 shows cell population having Annexin V^+ and PI^+ demonstrating late apoptosis.

Scanning Electron Microscopy (SEM):

The SEM images were taken for normal and apoptotic cells from the Scanning Electron Microscope as described by Fischer *et al.,* 2012 [23]. The Apoptotic/miRNA treated / control cells were added with freshly prepared 1ml of 2.5 % glutaraldehyde in PBS and incubated at 4ºC for 2-4 hrs. The culture petri dishes were thoroughly rinsed with PBS, three times for 10 minutes each. After primary fixation of Glutaraldehyde, 1 ml of 1% osmium tetroxide in dH_2O was added and incubated at room temperature for 1 hr. The cells were thoroughly rinsed with PBS, three times for 10 minutes each; then, cells were dehydrated through graded concentration of Acetone (30, 50, 70, 90, 95, and 100 %) for 5-15 minutes each. Then the cells were dried in a desiccator overnight. The samples were individually mounted on double-sided carbon tape, which was attached to a metal stab. These stabs were coated with electrically conducting metal, i.e., platinum, using a Sputter coater (JFC 1600; JEOL, Tokyo, Japan) at 20mA. The images were taken at different magnifications, i.e., 200X, 800X and 4000X, through Scanning Electron Microscope (JOEL-JSM6490LV).

qRT-PCR: HEK293T were harvested and total RNA was extracted using Pure Link RNA mini kit (Invitrogen, USA Cat No: 12183018A) according to the manufacturer's instruction. cDNA was synthesized using 1 µg total RNA using Proto Script® II First Strand cDNA Synthesis Kit (New England Biolabs Inc, USA Cat no: E6560S) as per the manufacturer instructions. qRT-PCR for MOAP1 was carried out using PowerUp™ SYBR™ Green Master Mix (Applied Biosystems Cat No: A25742). All the primers were procured through IDT technologies, USA with following sequences: MOAP1; F- 5' CACGAGCACTAGATCACGGCTGCTGGA 3' and R- CTGCCACACAGCAGCTCTGGGAGATGCC 3' [24], GAPDH; F- 5' ACATCGCTCAGACACCATG 3' and R- 5' TGTAGTTGAGGTCAATGAAGGG 3' [25]. The reactions were performed in an Agilent Aria Mx Real-Time PCR machine. The PCR conditions were as follows: UDG activation at 50ºC for 2 min, Hot start (Activation of SYBR Green) at 95^0C for 2 min followed by denaturation at 95^0C for 15 sec, annealing at 60^0C for 1 min for 40 cycles along with the melt curve analysis as per the machine protocol. To confirm specific amplification of the PCR product, dissociation curves were checked routinely, and fluorescence was measured continuously. The relative mRNA expression was normalized to that of GAPDH in the corresponding sample by $2^{-\Delta\Delta CT}$. The measurement was done in triplicates, and the results are presented at the means ±SEM.

Dual-luciferase reporter assays: To assess the ability of hcmv-miR-UL70-3p for binding with the 3' UTR of MOAP1, these assays were performed. Briefly, HEK293T cells were seeded in a 12-well plate (3×10^5 cells/well), and after 24 hrs, they were transfected along with 30nM of miR-UL70-3p mimic; its inhibitors;

both wild and deleted 3'UTR of MOAP1 cloned in pEZX-MT-06 vector using lipofectamine 3000 (Invitrogen) in triplicate wells. Luciferase activity was measured using the Dual-Luciferase Reporter assay system No E1910 (Promega Corporation, Madison, WI) in GloMax® Navigator Luminometer System, Promega as per manufacturer's protocol at 24 hrs post-transfection. All measurements were done in triplicate wells, and signals were normalized for transfection efficiency against the Renilla control. Data from three independent repetitions were presented as the mean ±SEM for the statistical analysis.

SDS-PAGE and Western blotting:

MOAP1 protein downregulation by hcmv-miR-UL70-3p was assessed by performing western blotting. Total protein from the different groups of samples (HEK293T cells) was extracted with the RIPA cell lysis buffer as per the protocol; protein quantification was done with the Bicinchoninic Acid (BCA) Protein Assay kit (G Biosciences, USA Cat No 786-570). The extracted proteins were separated by 10% acrylamide gel and transferred on the Immobilon-PVDF membrane (Millipore, Billerica, Massachusetts, USA). Western Blot analysis was performed using the primary antibody of MOAP1 (Novus Biologicals Cat No H00064112-M02) and its HRP conjugated secondary antibody (Santa Cruz Biotechnologies; Cat Nosc-516102) and β-actin primary antibody (Cell Signalling Technology Cat No 4970S) and the HRP conjugated secondary antibody (Cell Signalling Technology; Cat No 7074S). The immunoblot was visualized using an enhanced chemiluminescence detection kit (Amersham, GE Healthcare, USA), and the developed blots were observed using Chemiscope (Clinx, China). The detections were repeated in three independent experiments. The density of each protein band was read and quantified using Image J software ver 1.53e.

Statistical Analysis: Statistical analysis was performed using Graph Pad Prism 7.0. Software Inc (Graph Pad Software, San Diego, California, USA). Results are represented as mean ± SEM (Standard Error Mean) of at least three independent experiments unless stated otherwise. For simple comparisons, a two-tailed Student's t-test was used, and for multiple comparisons, two-tailed ANOVA was used. P-value inferior to 0.05 were considered as statistically significant (n=3).

Apoptotic induction and evaluation: Apoptosis was induced in HEK293T cells by treatment with H_2O_2 as described in Xiang et al., 2016 [26]. The brief outline for the procedure is different, as outlined below in fig1.

Results

1. Evaluation of the antiapoptotic effect of HCMV miR-UL70-3p on H_2O_2 induced apoptosis in HEK293T cells

To examine the anti-apoptotic activity of hcmv-miR-UL70-3p, we induced apoptosis in HEK293T cells through H_2O_2 as per the method described earlier [26] and evaluated its effect. Briefly, The HEK293T cells were divided into different groups, the first control group (without H_2O_2 treatment), the second group

(H_2O_2 treated); the third group (H_2O_2 and miR-UL70-3p) and the fourth group (H_2O_2, miR-UL70-3p along with miR-UL70-3p inhibitor). The HEK293T cells were seeded as per the protocol shown in fig. 1 for different experiments; the apoptotic nuclei counted through DAPI staining; Caspase 3/7 activity through Caspase-Glo 3/7 assay kit, and apoptosis by Flow cytometry. The cell membrane morphology differences were also examined through Scanning electron microscopy, and the results analysed through Image J software ver 1.53e.

a) 4',6-Diamidino-2-phenylindole (DAPI) staining:

All 4 groups of HEK293T cells were stained with 4',6-Diamidino-2-phenylindole (DAPI) and observed for the apoptotic nuclei at 20X magnification. Further, the cell's nuclear morphology and distributions were analyzed through ImageJ ver 1.53e. The 21.95 percent apoptotic cells were observed in the H_2O_2 treated cell group, while the cells transfected with miR-UL70-3p showed 7.4 percent apoptotic cells. So, a mean cumulative decrease of 14.54% apoptotic cells as compared to H_2O_2 treated cells. Further, in the cell group co-transfected with mir-UL70-3p and its inhibitor, the apoptotic cell percentage was 11.70 percent. A reversal of 4.29 percent of apoptosis was observed. This indicates that the miR-UL70-3p decreases the apoptosis induced by the H_2O_2 (Fig 2a & b).

b) Caspase-Glo 3/7 assay:

The antiapoptotic effect of miR-UL70-3p was evaluated by analysing the downregulation of caspase 3 and 7 through Caspase Glo 3/7assay, and the results obtained are shown in Fig 2b. Compared to the cell group treated with H_2O_2 (RLU $5.6X10^5$), with cell group transfected with miR-UL70-3p (RLU $3.3X10^5$) shows a significant decrease in the Cas3/7 activity, which suggest that the miRNA downregulated the apoptosis. Further, to confirm whether the observed down regulatory effect was due to miR-UL70-3p, the cell group was simultaneously transfected with miR-UL70-3p, and it increased the Cas3/7 activity to RLU $4.77\ X10^5$ (Fig 2c).

c) Flow Cytometry:

In addition to the above, we further evaluated the antiapoptotic effect of miR-UL70-3p through flow cytometry through Annexin-V and Propidium Iodide (PI). The cells were divided into 4 groups as mentioned above, and the apoptotic cell ratio in H_2O_2 treated group was 11.21 percent, whereas the cells group transfected with miR-UL70-3p was 3.74 percent (decrement of 7.47%). Once we transfected with the miRNA and its inhibitor, the apoptotic cell ratio became 9.59 percent. It clearly showed that whenever we simultaneously transfected the cells with miR-UL70-3p and its inhibitor, the effect of miR-UL70-3p was be reversed (Fig. 2d & e).

D) SEM analysis:

We further analyzed the morphological differences through the Scanning electron microscope for the cell groups by taking images at 200x, 800x and 4000X magnification in all the cells. Further, these images

were converted to histograms based on mean cell surface coverage area. The results showed that the reduced surface area due to the treatment of H_2O_2 was reversed when we transfected the cells with the miR-UL70-3p, suggesting that it decreased the process of apoptosis (Fig. 2f & g).

2. hcmv-miR-UL70-3p targets MOAP1, thereby regulates the H_2O_2 induced apoptosis?

Our earlier *in-silico* studies indicate that the proapoptotic gene, i.e., modulator of apoptosis 1 (MOAP1) was a potential target for hcmv-miR-UL70-3p.

a) miR-UL70-3p downregulates the mRNA expression of MOAP1: To examine if miR-UL70-3p downregulates the apoptosis by targeting the MOAP1 mRNA, we investigated the MOAP1 mRNA expression levels in the cells transfected with miR-UL70-3p and with H_2O_2. The results showed that the MOAP1 mRNA expression levels were significantly downregulated in the cells transfected with the miR-UL70-3p, compared to the cells treated with H_2O_2 only, suggesting that miR-UL70-3p downregulated the MOAP1 mRNA (Fig 3a). In order to confirm, MOAP1 downregulation was due to miR-UL70-3p. We analysed the MOAP1 mRNA expression in the cells simultaneously transfected with miR-UL70-3p and its inhibitor; the results showed that the mRNA expression levels were increased compared to the miR-UL70-p treated cells. These results confirm that the miR-UL70-3p can downregulate the mRNA levels of MOAP1.

b). miR-UL70-3p has potential binding sites in the 3'UTR of MOAP1

The above results confirm the downregulation of MOAP1 mRNA by hcmv-miR-UL70-3p; by performing the dual luciferase-based assays, we tried to prove the functionality of the binding site of miR-UL70-3p in the 3' UTR of the MOAP1. Our earlier studies show that the 3'UTR of MOAP1 has a potential binding site at the position of 527 for hcmv-miR-UL70-3p. The entire wild type (WT) and deleted (del) 3'UTR of MOAP1 dual-luciferase vector constructs were commercially procured and transfected in the cells to demonstrate the functionality of this binding site with miR-UL70-3p and measured for the luminescence. The results show that the luminescence was suppressed to 46.68% in the cells transfected with wild 3' UTR, compared to the 3'UTR deleted vector constructs, suggesting that the binding site predicted the 3'UTR region of MOAP1 was functional. Further, the luminescence was restored when we co-transfected with mir-UL70-3p inhibitor (Fig 3 b & c). These results confirm that the binding site at 527-549 of 3'UTR of MOAP1 is functional for hcmv-miR-UL70-3p.

c) MOAP1 protein suppression by hcmv-miR-UL70-3p:

We evaluated protein inhibition by this miRNA through western blotting once we confirmed the binding site for miR-UL-70-3p in the 3'UTR of MOAP1. The cell groups, as mentioned earlier, were taken and transfected with mir UL 70-3p and inhibitors and induced apoptosis through H_2O_2. After 6 hrs of H_2O_2 treatment, cells were lysed through RIPA buffers as explained in Materials and Methods, and the obtained protein concentrations were estimated through the BCA method. The results show that the cells transfected with miR-UL70-3p significantly downregulated the MOAP1 protein compared to the cells treated with H_2O_2 only. The downregulation of MOAP1 protein was reversed when the cells

simultaneously treated with the mir-UL70-3p and its inhibitor. Further, we compared the downregulation of MOAP1 protein levels by the miR-UL70-3p with the commercially available siRNA for MOAP1. The extent of MOAP1 downregulation was similar for both these molecules suggesting that the miR-UL70-3p downregulates the MOAP1 (Fig. 3d & e).

3. Comparison of MOAP1 mRNA and its protein inhibitions by the hcmv-miR-UL70-3p and siRNA of MOAP1:

After confirming the proapoptotic gene MOAP1 as a functional target for miR-UL70-3p, we further compared the extent of inhibition by miR-UL70-3p and the siRNA against MOAP1 on MOAP1 mRNA and its protein levels. The siRNA (27nt) was commercially procured and designed against 3' UTR of MOAP1 at position 38 to 66. The MOAP1 mRNA levels (Fig 4b & C) and its protein (Fig4d) inhibitions by the miRNA and siRNA were plotted, and we found that both significantly downregulated the MOAP1. However, the siRNA of MOAP1 inhibited 69.52% of mRNA and 35.67% of MOAP1 protein levels, while the miR-UL70-3p inhibited 46.66% and 21.05% respectively.

Discussion

In the present study, we demonstrated the antiapoptotic role of HCMV encoded miRNA miR-UL70-3p in *in vitro* studies by using HEK293T cells. Further, we ascribed the antiapoptotic activity of this miRNA ability to bind with the 3'UTR of the proapoptotic mRNA modulator of Apoptosis 1 (MOAP1) and thereby downregulating the MOAP1 protein. MOAP1 is a proapoptotic protein capable of initiating the apoptosis by interacting with Bax and RASSF1A. Its expression in different cells vary and is expressed in the adipose tissues, adrenal, blood, breast, colon, and comparatively at higher levels in the brain and heart. It interacts with apoptosis regulator Bcl-2 associated X protein (BAX) through its Bcl-2 homology 3 (BH3)-like motif and translocates the Bax on to the mitochondrial outer membrane leading to the polymerization. The Bax polymerization on the outer mitochondrial membrane results in to the increased permeability, thereby releases cytochrome C to the cytosol, initiating the mitochondrial dependent apoptosis [27–30]. At normal conditions, MOAP1 stays in an inactive conformation. However, it gets activated when it binds to RASSF1A and forms a death receptor complex after stimulated by TNFα and results in the opening of BH3 domain to allow to interact with Bax (Bcl-2 associated X protein). MOAP1 rapidly increases its concentration in the cytosol due to apoptotic stimuli and plays a pivotal role in initiating the mitochondrial-dependent apoptosis [31]. Targeting this proapoptotic protein by the HCMV miRNA miR-UL70-3p, HCMV downregulates the cellular apoptosis so that it can do productive infection at the early stages of infection. Being a *Herpesviridae* family of viruses, HCMV encodes 26 mature miRNAs, and they act in concert with the viral proteins in regulating the apoptosis for viral survival. Many research groups across the world actively engaged in deciphering the antiapoptotic role of HCMV miRNAs and understanding the fine tuning of HCMV proteins and miRNAs concordance in regulating apoptosis. The first HCMV miRNA reported to have antiapoptotic activity was miR-UL148D, and in that study, the authors demonstrated inhibition of IEX-1 induced apoptosis in HEK293 by ectopically expressing the miR-UL148D [17]. By performing *in silico* studies, we also reported the antiapoptotic activity to the HCMV miRNAs, miR-

UL70-3p and miR-UL148D [22], and predicted the proapoptotic gene, MOAP1 as a potential target for the miR-UL70-3p. In continuation, Kim et al. showed that ectopic expression of HCMV miRNAs, i.e., mir-UL36-3p, miR-US25-2p and miR-UL22A-3p downregulated the apoptosis by targeting the different caspases in Human Foreskin fibroblasts [19].

hcmv-miR-UL70-3p was first reported by Grey F et al in 2005 through northern blot analysis and further reported to be expressed both in the latent and lytic phases of HCMV infections [32]; however, the authenticity of this miRNA need to be established [33]. miR-UL70-3p reported to regulate the cellular apoptosis [22] and also reported to regulate focal adhesions, gap junctions, MAPK signalling and Erb pathway, thus effecting epithelial cell migration and adhesion [34]. It was reported that hcmv-miR-UL70-3p expression was different in different cells; for example, it was poorly induced in human embryonic lung cells (HELs); moderately in undifferentiated THP-1 cells and strongly in differentiated THP-1 cells (monocyte cell lines) [14]. Recent literature shows that an elevated expression of miR-UL70-3p in Glioblastoma cells suggest the cancer regulatory potential of this miRNA [35]. Further, Zhong et al. proposed that, in addition to human cells, the expression of hcmv-miR-UL70-3p and the other HCMV miRNAs miR-US4 is observed in the diseased human dental pulp. According to their bioinformatics study, the HCMV encoded miRNAs target human inflammation, antiviral mechanisms, and angiogenesis-related genes of the human. [36].

In this study we evaluated the antiapoptotic activity of miR-UL70-3p in HEK293T cells on H_2O_2 induced apoptosis. The apoptotic inhibition by this miRNA was measured as a percentage of apoptotic nuclei/apoptotic rate, inhibtion of effector Caspases 3/7 activity and membrane ruffling/blebbing in the cells. The fluorescence microscopic studies reveal that the apoptotic nuclei were significantly downregulated in the cells transfected with the miR-UL70-3p, and the inhibition was reversed when the treated cells were co-transfected along with miR-UL70-3p inhibitor(Fig. 2b). Further, we measured the apoptosis inhibition by the miRNA by measuring the effector Caspase(s) 3/7 levels, and these levels were downregulated in the cells transfected with miR-UL70-3p followed by H_2O_2 treatment, thereby showing inhibition of apoptosis when compared to the cells without the presence of this miRNA. The flow cytometry results confirm the antiapoptotic effect of miR-UL70-3p as there was a significant reduction of apoptotic cells (both early and late apoptotic nuclei) in the cells transfected with miR-UL70-3p. There was no significant reduction in early apoptotic cells but there was 7.3 percent reduction of apoptotic cells as observed in the late phase of apoptosis.

Our earlier *in silico* studies predicted that MOAP1 is the potential target for the mir-UL70-3p [22]; and has a single binding site in the 3'UTR at the position 527 to 549, to confirm this, we performed the dual-luciferase assays with both wild and deleted UTR's of MOAP1vectors tarsnfected along with miR-UL70-3p and measured the reduction in raw luminescence unit through luminometer. The results show 46.68 percent reduction in the luminescence observed in the cells transfected with the 3' UTR of MOAP1 compared to the deleted 3' UTR suggesting that the miR-UL70-3p bind to the site 527–549 and the binding ability of the miRNA is functional. Though the predicted target sequence was not completely complementary to the whole sequence of miR-UL70-3p; however, it was completely complementary to the

seed region of the miR-UL70-3p (2–8 position of the 5' miRNA). Human miRNAs hsa-miR-1228, miR-25 such as are also reported to target the MOAP1 and modulate the cellular apoptosis [24, 37]. These human miRNAs do not share any sequence homology with the hcmv-miR-UL70-3p (supplementary information S1) and the binding site is also not common (supplementary information S1), suggesting neither their sequences nor their binding sites were common.

The MOAP1 protein expression levels were examined in the groups treated with and without miR-UL70-3p transfection, and the results show the MOAP1 protein expression was decreased in the cells transfected with the mir UL 70-3p. This clearly indicates that the miR-UL70-p downregulating the MOAP1 protein levels by targeting the mRNA of MOAP1 in the 3' UTR region. We further compared the inhibitory action of this miRNA with the commercially available siRNA against the MOAP1 UTR region and found that though the extent of protein inhibition was more for the siRNA when compared to miR UL 70-3p.

Summing up the results it was clear that hcmv-miR-UL70-3p downregulates the H_2O_2 induced apoptosis in HEK293T cells by targeting the 3' UTR of MOAP1 mRNA. It was also clear that HCMV employs its miRNA machinery in regulating the various cellular processes, including apoptosis. However, more studies are required whether the proteins and miRNAs work synergistically or independently in regulating apoptosis. The miRNA-mediated regulation on the cellular hosts is spatiotemporal, which is decided by the virus to use these mechanisms to make a suitable environment for their survival.

Declarations

Funding Source: This work was supported by the grants from the Department of Biotechnology, Govt. of India (Project No: BT/PR14198/MED/29/980/2015); Department of Science & Technology- Science and Engineering Research Board (Project No: EEQ/2017/000438). Abhishek Pandeya is the recipient of Senior Research Fellowship from the Indian Council of Medical Research, New Delhi (45/28/2018/IMM/BMS Dated: 01.02.2019 IRIS Cell No. 2017-2392), and Raj Kumar Khalko is the recipient of the National Fellowship for Scheduled Tribes (Ministry of Tribal Affairs, New Delhi) fellowship (201819-NFST-JHA-02141).

Conflict of interest/ Competing interests: The authors declare no competing financial or conflict of interest.

Availability of data and material: Supporting data is included as electronic supplementary material.

Code Availability:

	Name	Source	Catalogue no	RRID number
Softwares				
1	ImageJ 1.53e	NIH	NA	SCR_001935
2	Graph pad Prism 7.0	Graphpad	NA	SCR_05807
Cell Lines				
3	HEK293T cell line	ATCC	CRL-3216	CVCL_0063
Vectors				
4	pEZX-MT06 MOAP1 WT	Genecopoeia	HmiT016794-MT06	SCR_003145
5	pEZX-MT06 MOAP1 DEL		Cmi000001-MT06	SCR_003145
General Chemicals				
6	DMEM	Gibco	11995065	NA
7	Fetal Bovine Serum, Brazil origin		10270106	NA
8	Antibiotic Antimycotic 100X		15240096	NA
9	DharmaFACT1	Dharmacon	T-2001-03	NA
10	Lipofectamine 3000	Invitrogen	L3000008	NA
Mimics, siRNAs and Inhibitor				
11	hcmv-miR-UL70-3p mimics	Ambion	**Assay ID:** MC11312, **Cat No:** 4464066	SCR_008406
12	hcmv-miR-UL70-3p inhibitor	Ambion	**Assay Id:** MH11312 **cat No:** 4464084	
13	siRNA of MOAP1	IDT	hs.Ri.MOAP1.13.1	SCR_001363
Kits				
14	Caspase Glo 3/7 assay,	Promega	G8090	NA
15	Dual Luciferase Reporter Assay		E1910	NA
16	Bicinchoninic Acid (BCA) Assay Kit	G Biosciences, USA	786-570	NA
17	Chemiluminescence detection kit (ECL)	GE Healthcare, USA	RPN2236	NA
Antibodies				
18	MAP-1 primary antibody	Novus	H00064112-M02	AB_1109361

		Biologicals		
19	m-IgGκ BP-HRP conjugated Secondary antibody	Santacruz Biotechnology	sc-516102	AB_2687626
20	β- actin primary antibody	Cell Signalling Technology	4970S	AB_330288
21	Anti-rabbit IgG, HRP-linked Antibody		7074S	AB_2099234

Authors' Contributions:

Conceptualization: Sunil Babu Gosipatala; **Methodology:** Sunil Babu Gosipatala, Abhishek Pandeya; **Formal analysis and investigation**: Sunil Babu Gosipatala, Abhishek Pandeya, Anup Mishra, Raj Kumar Khalko, Sukhveer Singh, Nishant Singh; **Writing - original draft preparation:** Sunil Babu Gosipatala, Abhishek Pandeya; **Writing - review and editing:** Sunil Babu Gosipatala, Abhishek Pandeya, Anup Mishra, Raj Kumar Khalko, Sanjay Yadav, Sudipta Saha, Sangeeta Saxena; **Funding acquisition:** Sunil Babu Gosipatala; **Resources:** Sunil Babu Gosipatala; **Supervision:** Sunil Babu Gosipatala, Sanjay Yadav.

Ethical and Biosafety Approvals:

This study was approved by Institutional Ethics Committee (**IEC No:** 19/BBAU-IEC/2016); Institutional Biosafety Committee (**IBSC No:** 01/IBSC/BBAU/2016), Babasaheb Bhimrao Ambedkar University, Lucknow - 226025 Uttar Pradesh (India).

Ethical and Biosafety Approvals:

This study was approved by Institutional Ethics Committee (**IEC No:** 19/BBAU-IEC/2016); Institutional Biosafety Committee (**IBSC No:** 01/IBSC/BBAU/2016), Babasaheb Bhimrao Ambedkar University, Lucknow - 226025 Uttar Pradesh (India).

Acknowledgements:

This work is supported by the grants from Department of Biotechnology, Govt of India (Project No: BT/PR14198/MED/29/980/2015); Department of Science and Technology- Scientific and Engineering Research Board Project (Project No: EEQ/2017/000438); Abhishek Pandeya received Indian Council of Medical Research-Senior Research Fellowship (45/28/2018/IMM/BMS IRIS Cell No.: 2017-2392), Raj Kumar Khalko received National Fellowship for Scheduled Tribes: (201819-NFST-JHA-02141). The authors would like to thank the University Sophisticated Instrumentation Centre, Babasaheb Bhimrao Ambedkar University, Lucknow, for using Scanning Electron Microscope for imaging and Council of Scientific and Industrial Research (CSIR), Indian Institute of Toxicology Research (CSIR-IITR), Lucknow, India for Flow Cytometry analysis.

References

1. Schottstedt V, Blümel J, Burger R, Drosten C, Gröner A, Gürtler L, Heiden M, Hildebrandt M, Jansen B, Montag-Lessing T, Offergeld R (2010) Human cytomegalovirus (HCMV)–revised. Transfus Med Hemother 37(6):365-375. https://doi.org/10.1159/000322141
2. Murphy E, Yu D, Grimwood J, Schmutz J, Dickson M, Jarvis M, Shenk T E (2003) Coding potential of laboratory and clinical strains of human cytomegalovirus. Proc Natl Acad Sci U S A 100(25):14976-14981. http://doi.org/1073/pnas.2136652100
3. Gatherer D, Seirafian S, Cunningham C, Holton M, Dargan, DJ, Baluchova K, Davison A J (2011) High-resolution human cytomegalovirus transcriptome. Proc Natl Acad Sci U S A 108(49):19755-19760. https://doi.org/10.1073/pnas.1115861108
4. Stern-Ginossar N, Weisburd B, Michalski A, Le VTK, Hein M Y, Huang S X, Weissman J S (2012) Decoding human cytomegalovirus. Science 338(6110):1088-1093. http://doi.org/10.1126/science.1227919
5. Dunn W, Chou C, Li H, Hai R, Patterson D, Stolc V, Liu F (2003) Functional profiling of a human cytomegalovirus genome. Proc Natl Acad Sci U S A 100(24):14223-14228. https://doi.org/10.1073/pnas.2334032100
6. Yu D, Silva M C, & Shenk T (2003) Functional map of human cytomegalovirus AD169 defined by global mutational analysis. Proc Natl Acad Sci U S A 100(21):12396-12401. http://doi.org/10.1073/pnas.1635160100
7. Shao Y, Qi Y, Huang Y, Liu Z, Ma Y, Guo X, Jiang S, Sun Z & Ruan, Q. (2017) Human cytomegalovirus miR-US4-5p promotes apoptosis via downregulation of p21-activated kinase 2 in cultured cells. Mol Med Rep 16(4):4171-4178. https://doi.org/10.3892/mmr.2017.7108
8. Benedict CA, Norris PS & Ware CF (2002) To kill or be killed: viral evasion of apoptosis. Nat Immunol 3(11):1013-1018. http://doi.org/ 1038/ni1102-1013
9. Goldmacher, V. S. (2005). Cell death suppression by cytomegaloviruses. Apoptosis 10(2):251-265. http:/doi.org/10.1007/s10495-005-0800-z
10. Poole E, Kuan WL, Barker R, & Sinclair J (2016) The human cytomegalovirus non-coding Beta2. 7 RNA as a novel therapeutic for Parkinson's disease–Translational research with no translation. Virus Res 212:64-69. http://doi.org/ 10.1016/j.virusres.2015.05.007
11. Maussang D, Verzijl D, Van Walsum, M, Leurs R, Holl J, Pleskoff O, Michel D, Dongen GAMSV, Smit, M J (2006) Human cytomegalovirus-encoded chemokine receptor US28 promotes tumorigenesis. Proc Natl Acad Sci U S A 103(35):13068-13073. http://doi.org/10.1073/pnas.0604433103
12. Guo X, Huang Y, Qi Y, Liu Z, Ma Y, Shao Y, Jiang S, Sun Z, Ruan Q (2015) Human cytomegalovirus miR-UL36-5p inhibits apoptosis via downregulation of adenine nucleotide translocator 3 in cultured cells. Arch Virol 160:2483-2490. https://doi.org/10.1007/s00705-015-2498-8
13. Lau B, Poole E, Krishna B, Montanuy I, Wills MR, Murphy E, Sinclair J (2016) The expression of human cytomegalovirus microRNA MiR-UL148D during latent infection in primary myeloid cells inhibits activin A-triggered secretion of IL-6. Sci Rep 6:31205. https://doi.org/10.1038/srep31205

14. Shen ZZ, Pan X, Miao LF, Ye HQ, Chavanas S, Davrinche C, McVoy M, Luo MH (2014) Comprehensive analysis of human cytomegalovirus microRNA expression during lytic and quiescent infection. PloS one 15(4):e0231909. https://doi.org/10.1371/journal.pone.0088531
15. Dunn W, Trang P, Zhong Q, Yang E, Van Belle C, Liu F (2005) Human cytomegalovirus expresses novel microRNAs during productive viral infection. Cell Microbiol 7(11):1684-1695. https://doi.org/10.1111/j.1462-5822.2005.00598.x
16. Shao Y, Qi Y, Huang Y, Liu Z, Ma Y, Guo X, Jiang S, Sun Z, Ruan Q (2016) Human cytomegalovirus-encoded miR-US4-1 promotes cell apoptosis and benefits discharge of infectious virus particles by targeting QARS. J Biosci 41(2):183-192. https://doi.org/10.1007/s12038-016-9605-1
17. Wang YP, Qi Y, Huang YJ, Qi ML, Ma YP, He R, Ji YH, Sun ZR, Ruan Q (2013) Identification of immediate early gene X-1 as a cellular target gene of hcmv-mir-UL148D. Int J Mol Med 31(4):959-966. https://doi.org/10.3892/ijmm.2013.1271
18. Liu Y, Pan J, Liu L, Li W, Tao R, Chen Y, Li H, Shang S (2017) The influence of HCMV infection on autophagy in THP-1 cells. Medicine (Baltimore) 96(44):e8298. https://doi.org/1097/MD.0000000000008298
19. Kim S, Seo D, Kim D, Hong Y, Chang H, Baek D, Kim VN, Lee S, Ahn K (2015) Temporal landscape of microRNA-mediated host-virus crosstalk during productive human cytomegalovirus infection. Cell Host Microbe 17(6):838-851. https://doi.org/10.1016/j.chom.2015.05.014.
20. Liu Y, Pan J, Liu L, Li W, Tao R, Chen Y, Li H, Shang S (2017) The influence of HCMV infection on autophagy in THP-1 cells. Medicine (Baltimore) 96(44):e8298. https://doi.org/10.1097/MD.0000000000008298
21. Fan J, Zhang W, Liu Q (2014) Human cytomegalovirus-encoded miR-US25-1 aggravates the oxidised low density lipoprotein-induced apoptosis of endothelial cells. Biomed Res Int 2014:531979. https://doi.org/10.1155/2014/531979
22. Babu SG, Pandeya A, Verma N, Shukla N, Kumar RV, Saxena S (2014) Role of HCMV miR-UL70-3p and miR-UL148D in overcoming the cellular apoptosis. Mol Cell Biochem 393:89-98. https://doi.org/10.1007/s11010-014-2049-8
23. Fischer ER, Hansen BT, Nair V, Hoyt FH, & Dorward DW (2012) Scanning electron microscopy. Curr Protoc Microbiol 24(1):2B.2.1-2B.2.47 https://doi.org/10.1002/9780471729259.mc02b02s25
24. Yan B, Zhao JL (2012) miR-1228 prevents cellular apoptosis through targeting of MOAP1 protein. Apoptosis 17:717-724. https://doi.org/10.1007/s10495-012-0710-9
25. Zuo Q, Wu R, Xiao X, Yang C, Yang Y, Wang C, Lin L, Kong AN (2018) The dietary flavone luteolin epigenetically activates the Nrf2 pathway and blocks cell transformation in human colorectal cancer HCT116 cells. J Cell Biochem 119(11):9573-9582. https://doi.org/10.1002/jcb.27275
26. Xiang J, Wan C, Guo R, Guo D. (2016) Is hydrogen peroxide a suitable apoptosis inducer for all cell types? Biomed Res Int 2016:7343965. https://doi.org/10.1155/2016/7343965
27. Tan KO, Fu NY, Sukumaran SK, Chan SL, Kang JH, Poon KL, Chen BS, Victor CY (2005) MAP-1 is a mitochondrial effector of Bax. Proc Natl Acad Sci U S A 102(41):14623-14628.

https://doi.org/10.1073/pnas.0503524102

28. Baksh S, Tommasi S, Fenton S, Victor CY, Martins LM., Pfeifer GP, Latif F, Downward J, Neel BG (2005) The tumor suppressor RASSF1A and MAP-1 link death receptor signaling to Bax conformational change and cell death. Mol Cell 18(6):637-650. https://doi.org/10.1016/j.molcel.2005.05.010
29. Vos MD, Dallol A, Eckfeld K, Allen NP, Donninger H, Hesson LB, Calvisi D, Latif F, Clark GJ (2006) The RASSF1A tumor suppressor activates Bax via MOAP-1. J Biol Chem 281(8):4557-4563. https://doi.org/10.1074/jbc.M512128200
30. Fu N Y, Sukumaran S K, & Victor CY (2007) Inhibition of ubiquitin-mediated degradation of MOAP-1 by apoptotic stimuli promotes Bax function in mitochondria. Proc Natl Acad Sci U S A 104(24):10051-10056. https://doi.org/10.1073/pnas.0700007104
31. Foley CJ, Freedman H, Choo S L, Onyskiw C, Fu N Y, Victor C Y, Tuszynski J, Pratt JC, Baksh S (2008) Dynamics of RASSF1A/MOAP-1 association with death receptors. Mol Cell Bio 28(14):4520-4535. http://doi.org/ 10.1128/MCB.02011-07
32. Grey F, Antoniewicz A, Allen E, Saugstad J, McShea A, Carrington J C & Nelson J (2005) Identification and characterization of human cytomegalovirus-encoded microRNAs. J Virol 79(18):12095-12099. http://doi.org/ 1128/JVI.79.18.12095-12099.2005
33. Zhang L, Yu J, Liu Z (2020) MicroRNAs expressed by human cytomegalovirus. Virol J. 17(1):34. http://doi.org/10.1186/s12985-020-1296-4
34. Naqvi AR, Shango J, Seal A, Shukla D, Nares S (2018) Viral miRNAs Alter Host Cell miRNA Profiles and Modulate Innate Immune Responses. Front Immunol. 9:433. http://doi.org/10.3389/fimmu.2018.00433
35. Ulasov IV, Kaverina NV, Ghosh D, Baryshnikova MA, Kadagidze ZG, Karseladze AI, Baryshnikov AY, Cobbs CS (2017) CMV70-3P miRNA contributes to the CMV mediated glioma stemness and represents a target for glioma experimental therapy. Oncotarget 8(16):25989-25999. https://doi.org/10.18632/oncotarget.11175
36. Zhong S, Naqvi A, Bair E, Nares S, Khan AA (2017) Viral MicroRNAs Identified in Human Dental Pulp. J Endod 43(1):84-89. http://doi.org/10.1016/j.joen.2016.10.006
37. Wu T, Chen W, Kong D, Li X, Lu H, Liu S, Wang J, Du L, Kong X, Huang X, Lu Z (2015) miR-25 targets the modulator of apoptosis 1 gene in lung cancer. Carcinogenesis 36(8):925-935. https://doi.org/10.1093/carcin/bgv068

Figures

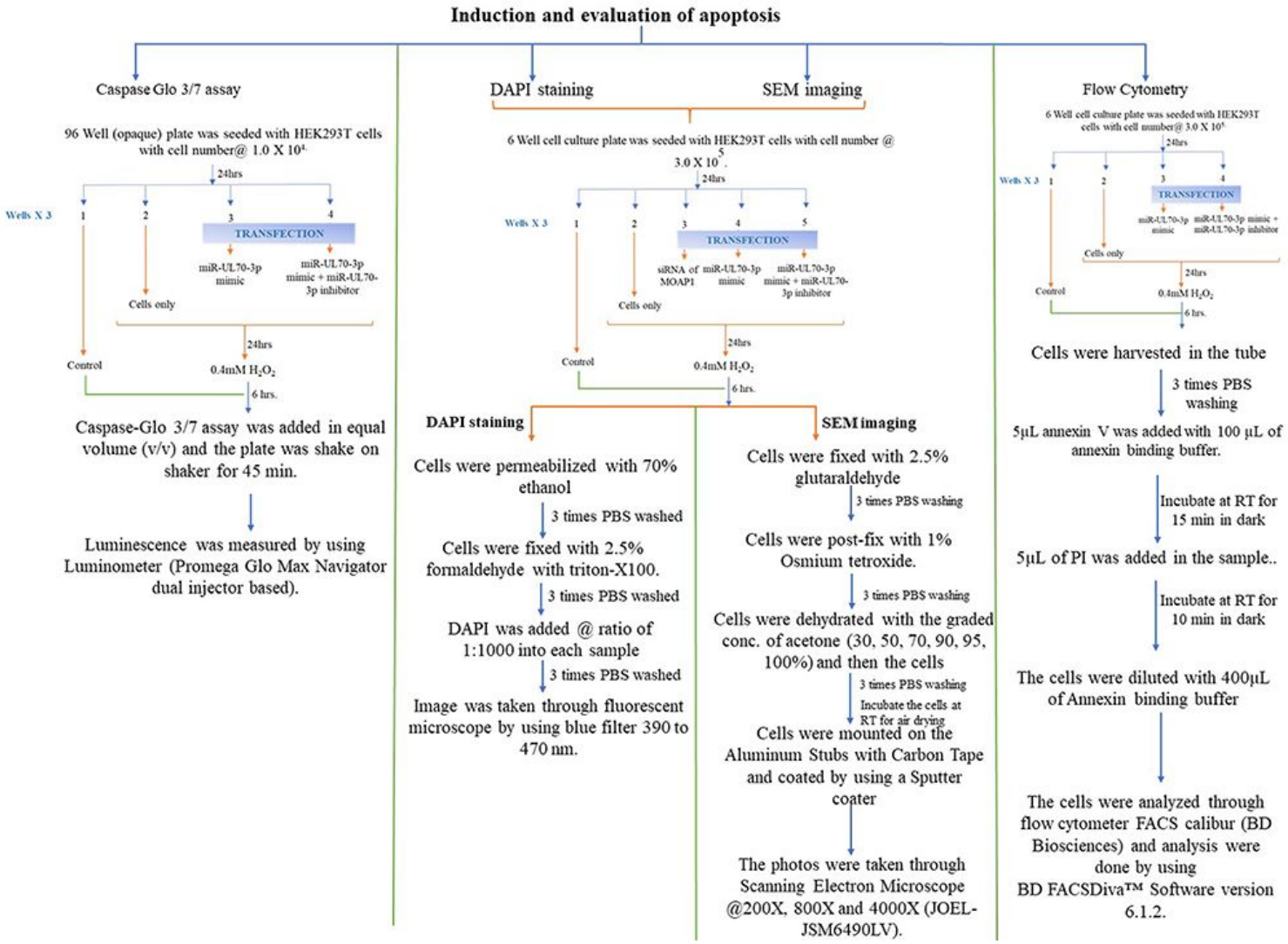

Figure 1

Flow diagram for the procedure followed for the induction and evaluation of apoptosis in HEK293T cells

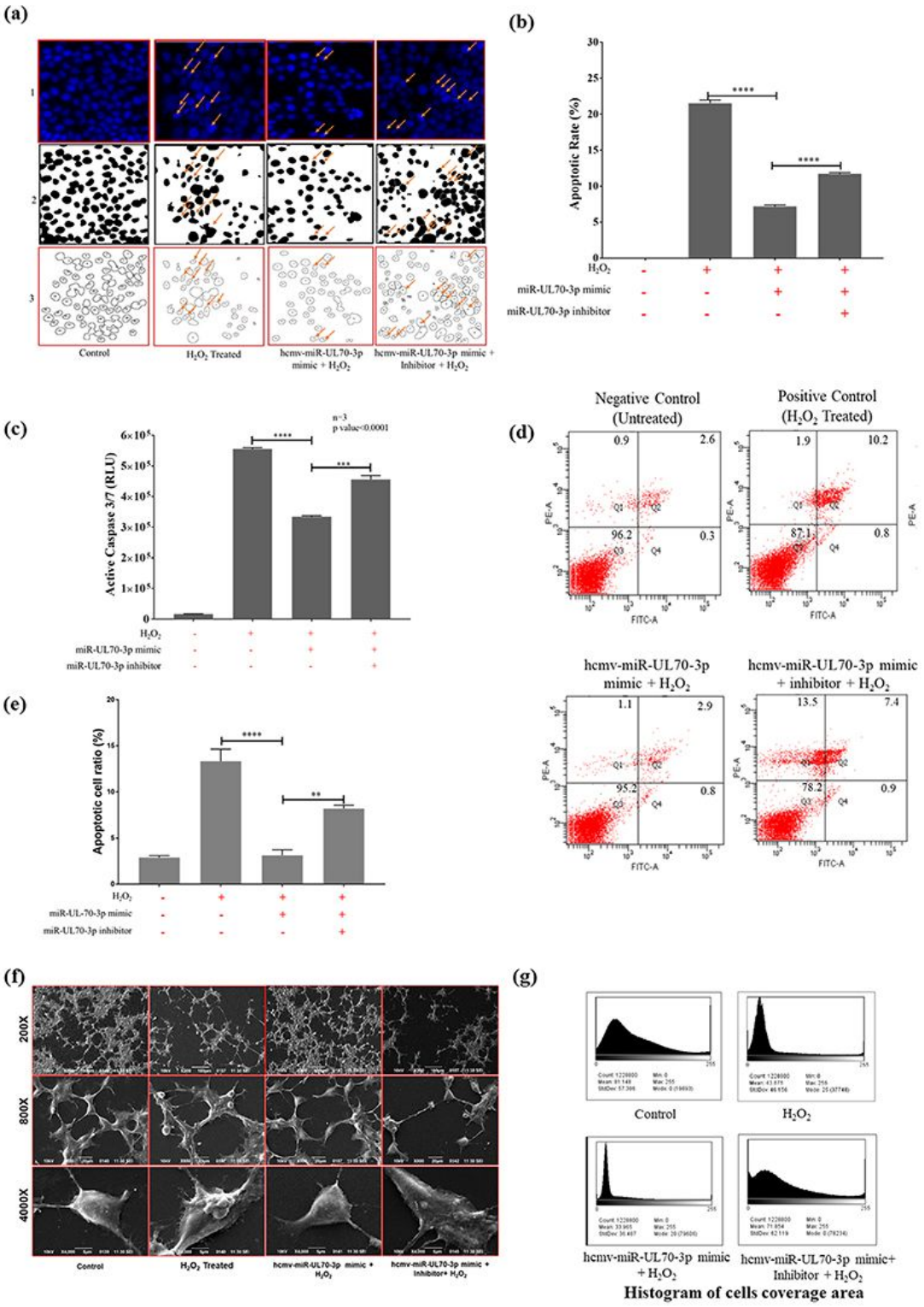

Figure 2

Evaluation of antiapoptotic effects of miR-UL70-3p on H2O2 induced apoptosis: (a) Antiapoptotic effect of hcmv-miR-UL70-3p through DAPI (b) Percentage of decrement of apoptotic nuclei in the cells group transfected with miR-UL70-3p. (c) Effect of miR-UL70-3p on the expression of Cas3/7 activity through Caspase 3/7 Glow assay. (d) Antiapoptotic effect of miR-UL70-3p through Flowcytometry by using Annexin V and Propidium Iodide. Evaluation of hcmv-miR-UL70-3p on H2O2 induced cellular apoptosis in

HEK293T cells. The cells were stained with Annexin-V Alexa Fluor 488 conjugated (Annexin-V) and Propidium Iodide (PI) and analyzed the apoptosis on a flow cytometer. The primary setting of FACS analysis was based on the fluorescence from blank/Unstained/ singly stained cells with Annexin V and PI, respectively. Fine tuning was based on the cell distributions of the different experimental groups. The assay was performed in triplicate wells (n=3). (e) Graphical representation of apoptotic cell rate for different sets of experiments. Data from three independent experiments were used for statistical analysis. (f) Treated and transfected HEK293T cells were analyzed for morphological changes through the Scanning Electron Microscope at a magnification of 200X, 800X and 4000X. Differences were seen as the blebbing, shrinking on the cell surface. The HEK293T cells transfected with hcmv-miR-UL70-3p treated with H_2O_2 shows lesser apoptotic cells with less blebbing/ membrane disintegration. In transfected cells with mimics and its inhibitor again, the cell rupture/ membrane disintegration/ blebbing was seen. (g) The histogram shows the mean value of the cell surface coverage area for different sets of experiments based on the Scanning Electron Microscope.

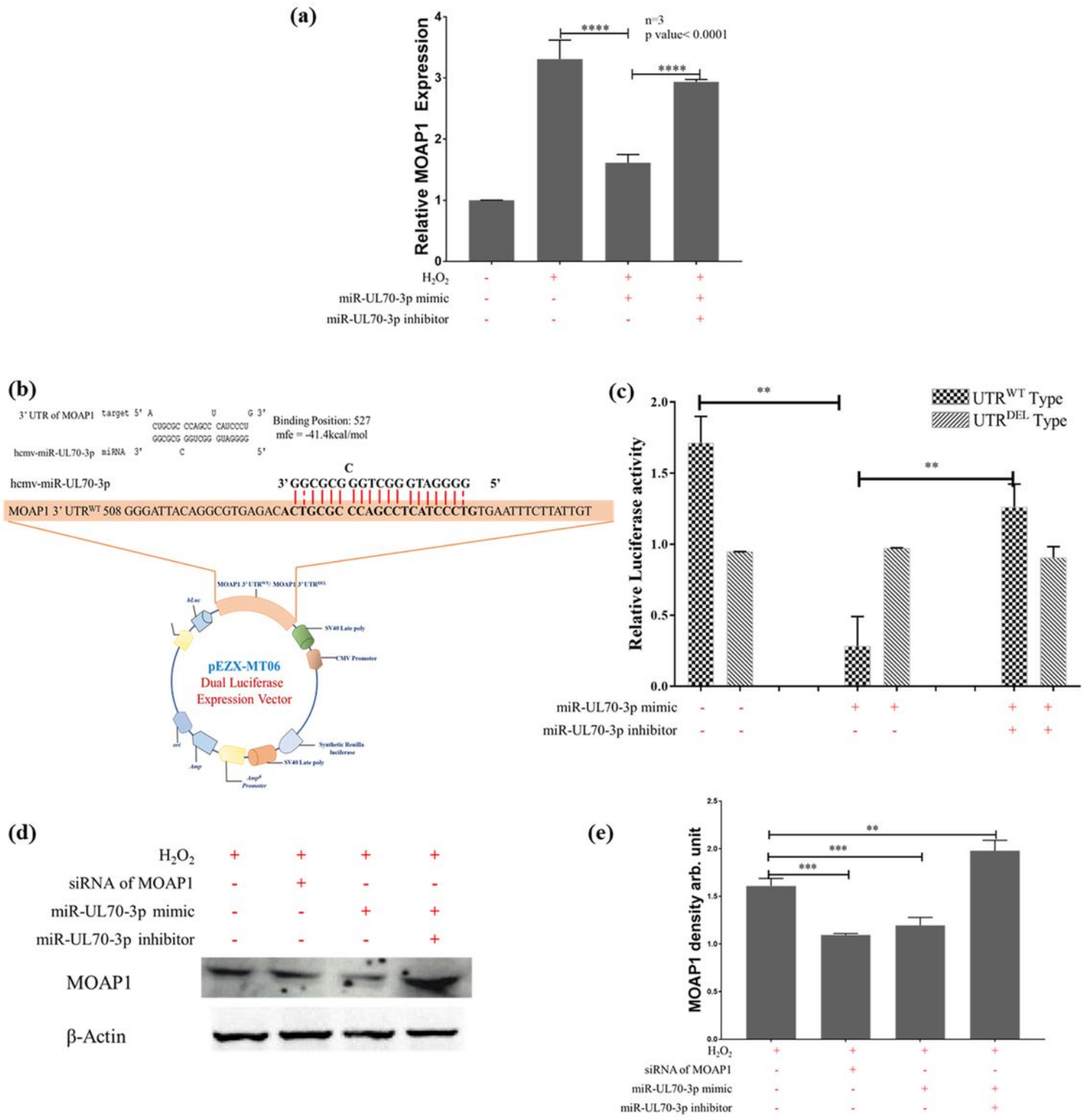

Figure 3

(a) Effect of hcmv-miR-UL70-3p on the expression of MOAP1 mRNA. Each sample was analysed in triplicates. Results are expressed as the fold change (2-ΔΔCt) in treatment groups relative to the control group (± SEM; n=3; P value=0.005). (b) Confirming the binding site at position 527 in the 3' UTR of MOAP1 for hcmv-mir-UL70-3p. RNA hybrid results were showing the binding site (mfe of -41.4 kcal/mol). The pEZX-MT06 (Genecopoeia) expression vector constructs (both wild and mutant UTR's) (c) The results

of dual Luciferase Reporter assay showing the inhibition of relative luminescence confirming the binding of miR-UL70-3p. Data collected from the three independent experiments were statistically analysed by two-way ANOVA, n=3, and P-value is <0.0001. (d) MOAP1 protein levels were detected by Western Blot. Relative protein expression was calculated based on densitometric analysis of band intensities. The blot image shown was cropped with no further manipulations. The Blot shows the western blotting result for β-actin and MOAP1. (e) Graphical representation of the expression of MOAP1 with the effect of hcmv-miR-UL70-3p. (The data expressed as means ±SEM; p value= 0.0003; n= 3).

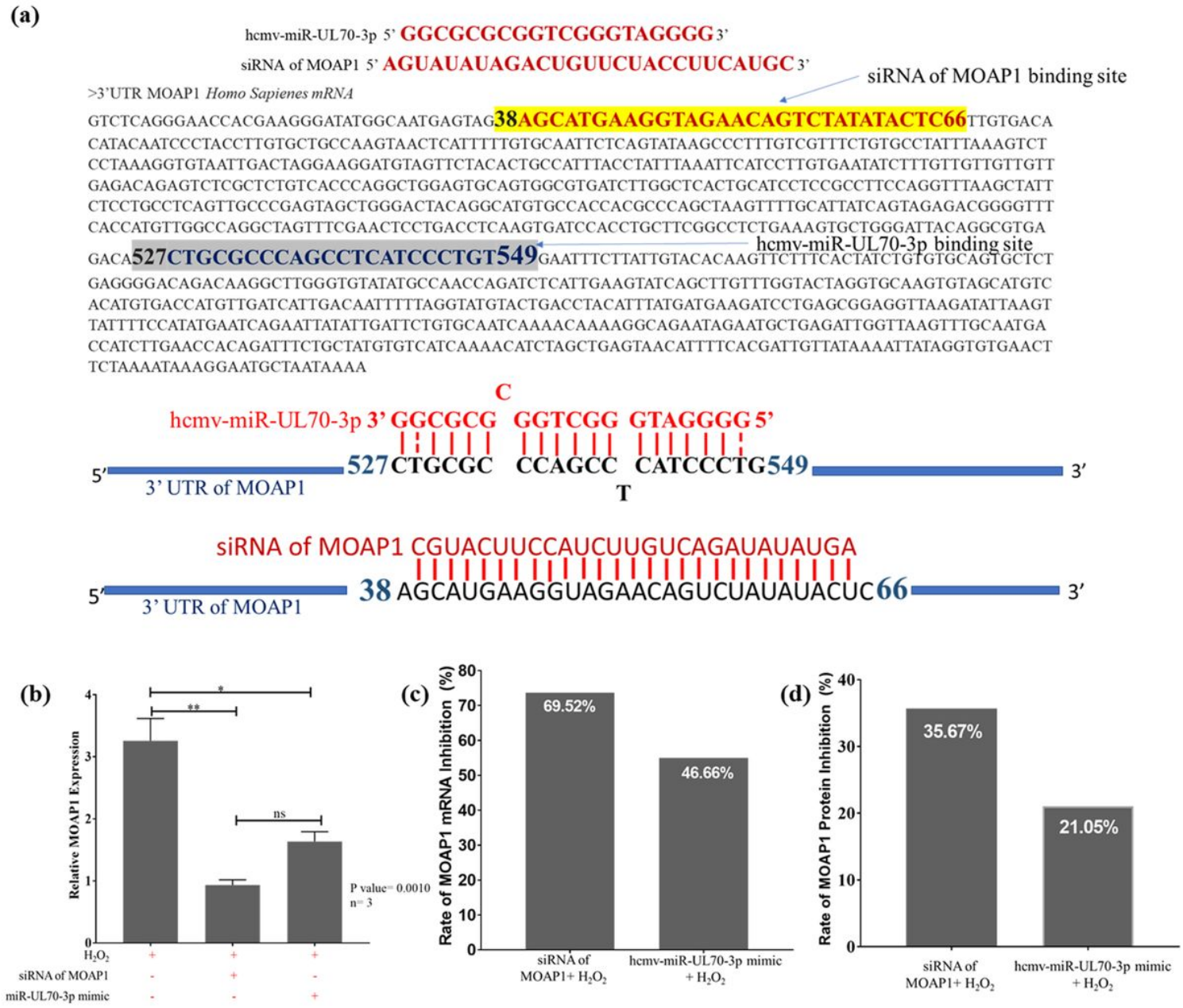

Figure 4

(a) Binding sites for commercially available siRNA of MOAP1 and hcmv-miR-UL70-3p and the in the 3' UTR of MOAP1 (988 bp) at positions 38 to 66 bp and 527 to 546 bp (b) Effect of hcmv-miR-UL70-3p and siRNA on the expression of MOAP1 mRNA. Each sample was analysed in triplicate. Results are expressed

as the fold change (2-ΔΔCq) in treatment groups relative to the control group (± SEM; n=3; P value=0.005). (c) Comparative MOAP1 mRNA inhibitions by the miR-UL70-3p & siRNA of MOAP1 to the positive control. (d) Comparative MOAP1 protein inhibition by the miR-UL70-3p & siRNA of MOAP1 to the positive control.

Supplementary Files

This is a list of supplementary files associated with this preprint. Click to download.

- S1.tif
- SupplimentaryInformationS2AnalysisFiles.xlsx